24th INTERNATIONAL CONGRESS ON SOUND AND VIBRATION
23–27 July 2017, London

NUMERICAL PREDICTION OF PERFORATED TUBE ACOUSTIC IMPEDANCE

G. Pradeep, T. Thanigaivel Raja, D.Veerababu and B. Venkatesham

Department of Mechanical and Aerospace Engineering, Indian Institute of Technology Hyderabad, Hyderabad, Telangana, 502285, India.
Email: venkatesham@iith.ac.in

S. Ganesan

ABES, GTRE, Bangalore, India.

The use of perforated sheets is very common in noise control applications such as mufflers, aero-engines, building acoustics and heating ventilation and air-conditioning systems. The acoustic performance of these liners is expressed mathematically in terms of its impedance. There is a great amount of literature available to estimate the liner impedance. Most of the models are semi-empirical in nature and derived from experimental studies. Geometric parameters like orifice diameter, plate thickness, cross-sectional dimension, hole distribution pattern, operating flow conditions and sound pressure levels play a critical role in perforated tube impedance estimations. In this work, a numerical methodology was developed based on Finite-Element Methods, to estimate the impedance of perforated plate and validated with existing literature results for stationary flow conditions. Perforated plate inside the circular tube is considered as a computational acoustic domain. Plane wave excitation is applied as the inlet boundary condition at one end of the tube, anechoic termination is applied as the outlet boundary condition and the rest of the exterior domain is assumed to be acoustically rigid. This methodology has been extended to evaluate the impedance of perforated tubes. Parametric studies are conducted to study the curvature effect of perforated tubes on impedance, by changing the tube diameter.

Keywords: perforate plate impedance, curvature effect, stationary flow, finite element model

1. Introduction

Perforated sheets are sheets with the pattern of holes, punched or stamped on them and are drawn into plates and tubes. They can absorb sound for a wide range of frequencies and are typically found in mufflers, aero engines, building acoustics, heating ventilation and air-conditioning systems (HVAC) etc. The perforated liners of aero engines and gas turbines also assist in the dissipation of heat, by allowing cool air to flow through them, which in turn help in the sound dissipation process. On account of these impressive features of perforated sheets, there is a greater research interest in quantifying their acoustic performance capabilities for moving and stationary mediums.

In the literature, sound absorption capabilities of perforated sheets have been studied for moving and stationary mediums through experimental, theoretical and numerical methods. A review of the liner impedance models can be found in [1, 2]. Extensive research has been carried out for perforated sheets with moving medium as compared to stationary medium. Primarily, for the moving medium, an experimental investigation has been carried out in NASA Langley Research Centre and by Bellucci et al. [3-6]. Further, theoretical analysis of the perforated liner for moving medium to study the curvature effects was carried out by Hughes and Dowling [7]. Furthermore, numerical methods employing Large eddy simulation (LES) and Finite element methods (FEM) have been used to study the acoustic performance of single hole liner configuration for moving medium [3, 8-11]. Most of the authors adopted the configuration which is same as experimental setup used by Bellucci et al. [6] in LES simulations for different flow conditions. Jones et al. [3] used FEM and an experimental setup together to assess the acoustic impedance of liner for moving medium. Andreini et al. [11] assessed the use of theoretical, FEM and LES methods for determining the acoustic impedance of liner for the moving medium. The study revealed that theoretical model is beneficial in the preliminary stage for selecting the liner porosity; LES shall be used to study fluid dynamic details of the damping process with high accuracy, and FEM in combination with theoretical model shall be used to study the overall acoustic behaviour.

For a stationary medium, minimal research has been carried out for numerical analysis of perforated sheets. Empirical models based on experimental results for stationary flow condition is evidenced in [12-13]. An Effort to theoretically study the acoustic impedance of liner for a stationary flow is witnessed in [14]. However, FEM has been rarely employed to study for stationary medium. Thus, it motivates for current study which develops a numerical methodology based on FEM for estimating the acoustic impedance of perforated plate with single hole, multiple hole and cylindrical liners.

The rest of the paper is organised as follows. Section 2 presents with the numerical model to estimate the acoustic impedance of a perforated plate with single hole, multiple holes and a cylindrical liner with a single hole. Section 3 presents with the discussion of the results. Finally, Section 4 provides with the summary.

2. Numerical Model

To calculate the impedance of a single hole under no flow condition, a typical impedance tube configuration as shown in Fig. 1 was modelled and the results were validated with theoretical models available in the literature. Another sample configuration with multiple holes is simulated in virtual impedance tube model and the acoustic impedance results are compared with existing single hole based models. To study the effect of curvature, a concentric tube resonator (CTR) was modelled with a single hole. Parametric studies were conducted by varying the inner tube diameter, hole diameter and liner wall thickness.

2.1 Geometry

The computational domain of impedance tube with a single hole is shown in Fig. 1. For multiple hole sample, a 4x4 array of holes with 15 mm spacing as shown in Fig. 2 is used in impedance tube modelling.

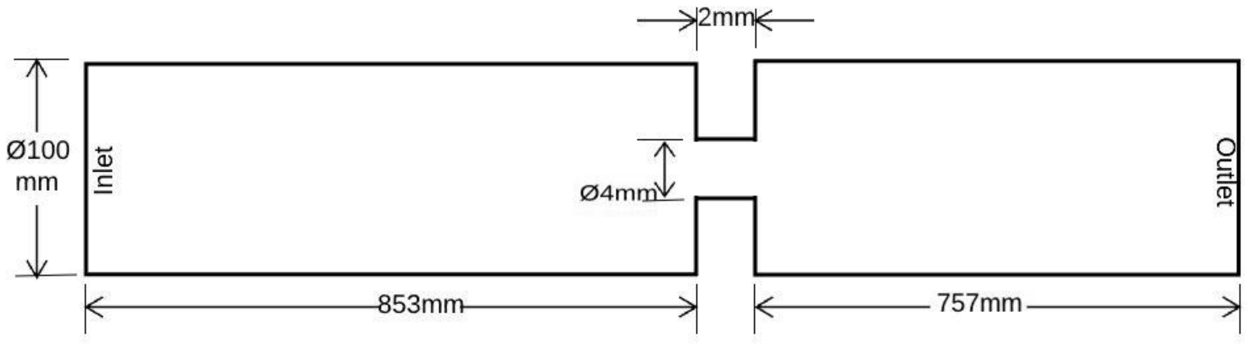

Figure 1: Computational domain of impedance tube with single hole sample

Figure 3 shows the computational domain for CTR with a single hole. The fixed dimensions of the CTR tube are D = 150 mm, l = 800 mm, L = 450 mm, l_1 = 250 mm and the remaining dimensions, inner tube diameter (d), hole radius (d_h) and liner thickness (t) were varied and as shown in Table 1.

Underline represents the default values of the model. The plane wave cut-off frequency for the largest inner tube diameter in CTR is 3186 Hz.

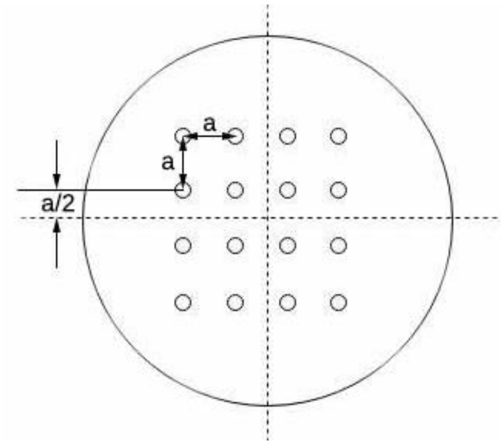

Figure 2: Multiple hole sample configuration with 16 holes with spacing 'a'

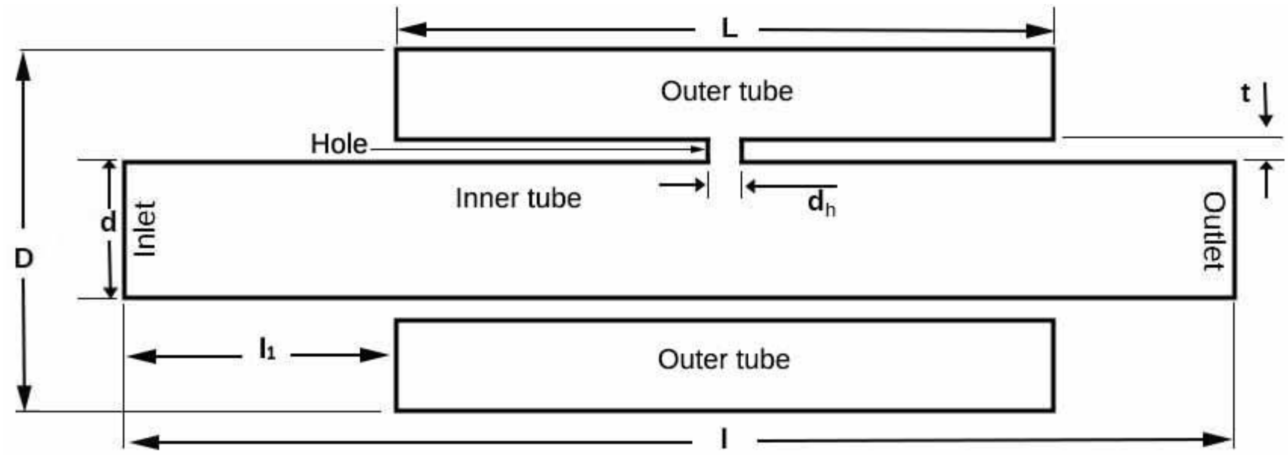

Figure 3: Computational domain of CTR with single hole

Table 1: Dimensions used in parametric studies

Parameter	Dimension in mm
Inner pipe diameter (d)	62.5, 50, 25, 12.5
Hole diameter (d_h)	1, 4, 10
Liner wall thickness (t)	1, 2, 5

2.2 Meshing

Triangular elements were used to mesh the 2D surfaces and tetrahedral mesh was used for 3D elements. To maintain uniform mesh in all the models, the number of nodes were kept constant around the edges. The number of nodes around the hole circumference is 25 and the number of nodes on hole thickness is 4. The maximum length of the element in the mesh is 22 mm and the corresponding valid maximum frequency is 3864 Hz for a chosen speed of sound 340 m/s. Standard mesh quality checks were performed [15].

2.3 Finite Element Model

The complete meshed model of the impedance tube with a single hole is shown in Fig. 4.

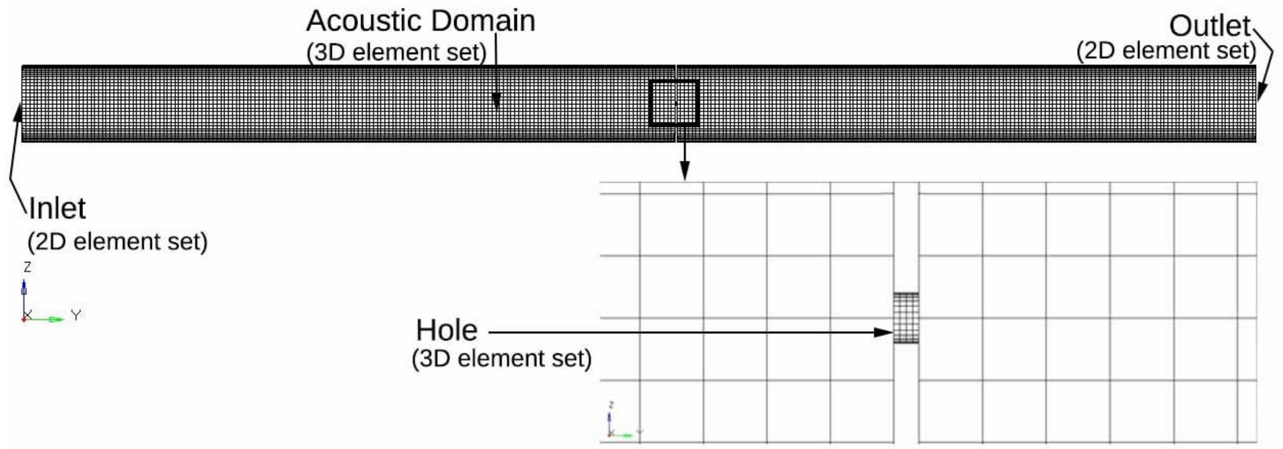

Figure 4: Meshed model of impedance tube with single hole sample

The mesh consists of 2D elements at the inlet and outlet surfaces as shown in Fig. 4. and boundary conditions were applied on these elements. The acoustic domain contains 3D tetrahedral elements with air as the medium. 2D elements exist at the hole inlet and outlet surfaces which were used to monitor the pressure and average velocity. Figure 5 shows the meshed model of CTR with a single hole. 2D elements exist at the inlet and outlet of tube and hole surfaces.

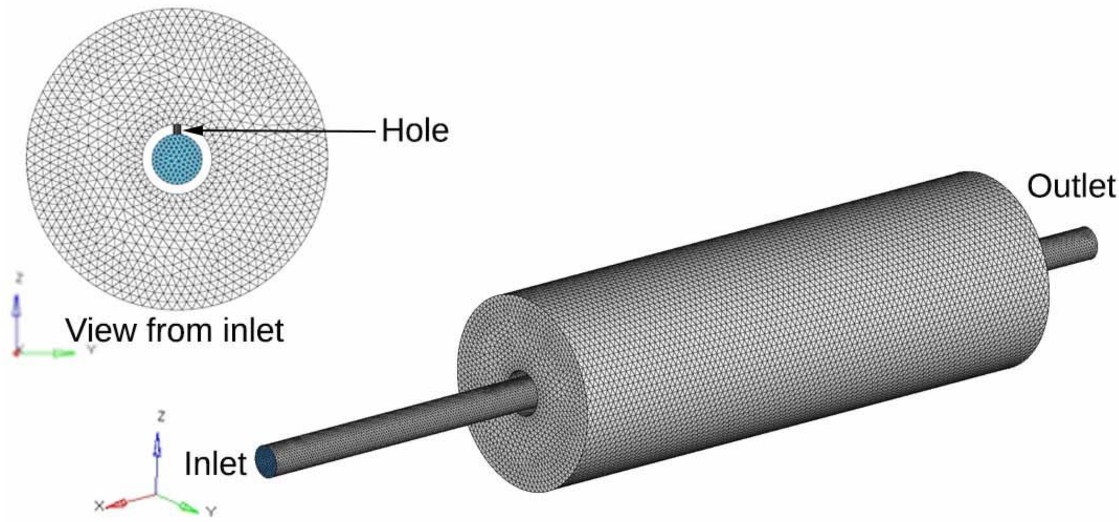

Figure 5: Meshed model of CTR with single hole

A direct frequency response analysis is performed for a frequency range 0-1000 Hz with a step of 10 Hz in a commercial software Actran [16]. The maximum frequency was selected in such a way that only plane wave mode propagates for all chosen configurations. A plane mode excitation of 1 Pa is given at the inlet and a non-reflecting boundary condition is given at the outlet surface.

Sample specific acoustic impedance is defined as a ratio of the pressure difference across the sample and average velocity on inlet sample surface as in Eq. (1).

$$z = \frac{p_1 - p_2}{\bar{v}} \tag{1}$$

where z is the impedance, $\bar{v}$ is the average velocity over the sample inlet surface, and p_1, p_2 are the pressures at the inlet and outlet of the sample surface, respectively.

3. Results

3.1 Calculation of end correction coefficient

Figure 6 shows a comparison of resistance and reactance for a single hole configuration between FEA and theoretical model as given in Eq. (2) [17].

$$\zeta = \frac{0.006 + jk \times (t + 0.75 \times d_h)}{\sigma} \tag{2}$$

where the normalised resistance is a constant value for a specific porosity, k is the wave number, t is the thickness of hole, d_h is the diameter of the hole and σ is the porosity. In this case, the porosity is one since only single hole exists. The end correction constant in Eq. (2) was 0.75. But, there is a disagreement in reactance as shown in Fig. 6 due to end correction value, so it is estimated again based on the numerical results by equating the normalised reactance. The new end correction coefficient for the theoretical model should be 0.7.

The calculated end correction value is used in theoretical impedance model for multiple hole configuration. It can also be observed that the value of resistance is much lesser than the reactance values in both the methods. So the contribution of resistance is ignored in the analysis.

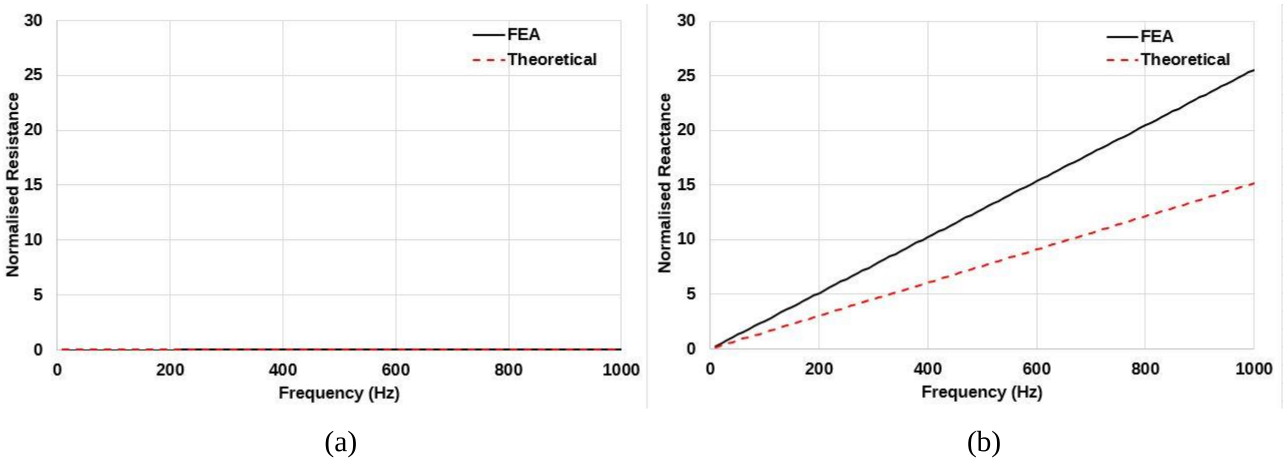

Figure 6: Comparison between FEA and theoretical results (a) normalized resistance (b) normalised reactance

In case of multiple hole configuration, the total sample impedance is calculated in terms of single hole impedance (z_s) as

$$Z = \frac{z_s}{n} \times \left(\frac{d}{d_h}\right)^2 \tag{3}$$

where Z is the total impedance, n is the number of holes, d is the inner tube diameter and d_h is the hole diameter. The numerically calculated total impedance of multiple holes is compared with the impedance of single hole model by taking porosity into consideration as given in Eq. (2) and results are shown in Fig. 7. The porosity (σ) of unit cell configuration can be calculated from Fig. 2 as $\sigma = (\pi/4) \times (d_h^2/a^2)$. The porosity ($\sigma'$) for the same configuration considering all holes can be written as

$$\sigma' = OAR = \frac{n \times \frac{\pi}{4} \times d_h^2}{\frac{\pi}{4} \times d^2} \tag{4}$$

where *OAR* is the open area ratio. It can be seen from Fig. 7 that if the multiple hole configuration is not a regular pattern, then estimating the impedance based on a single hole with porosity (Eq. 2) using unit cell configuration is not appropriate.

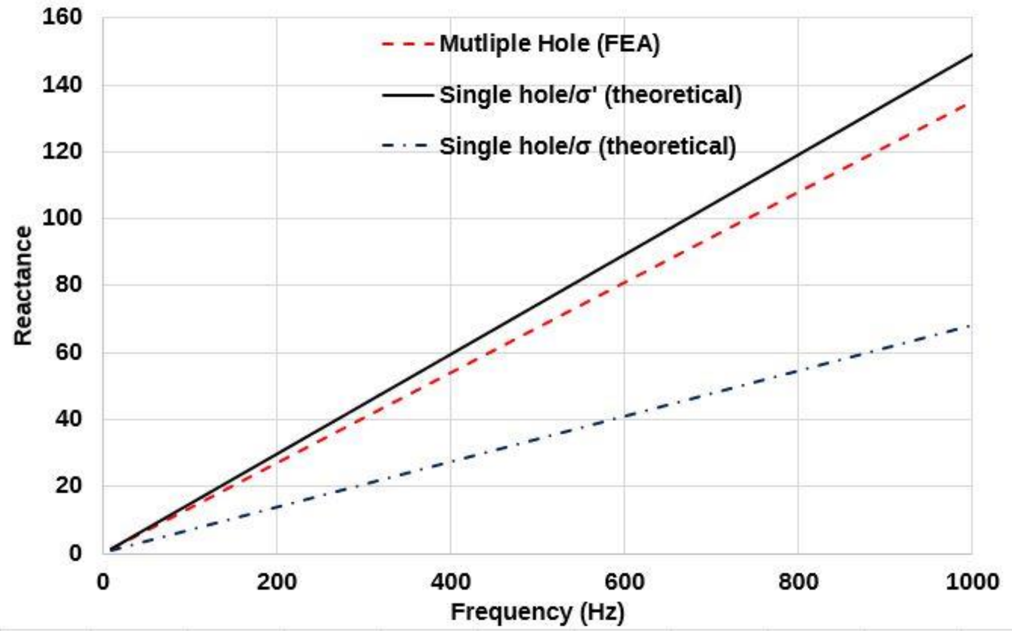

Figure 7: Comparison of reactance of multiple hole FEA model and theoretical model

3.2 Curvature Effect

Figure 8 shows the reactance of four different configurations of CTR. The inner tube diameter is varied as mentioned in Table 1. It can be observed from Fig. 8 that the variation in reactance value is marginal with the radius of curvature. It is due to the fact that the curvature effects will become significant in the presence of higher order modes [6]. In the present analysis only plane wave propagation exists in the considered frequency range of interest. This shows consistency that the curvature effects can be observed at higher order modes as mentioned in [6].

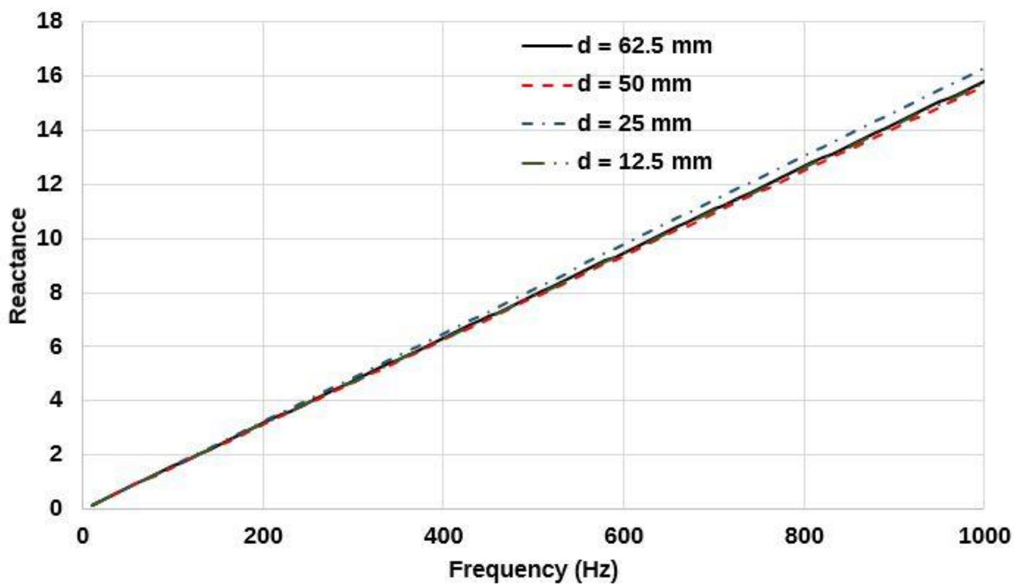

Figure 8: Variation of reactance with inner tube diameter (d) in CTR configuration

3.3 Parametric studies

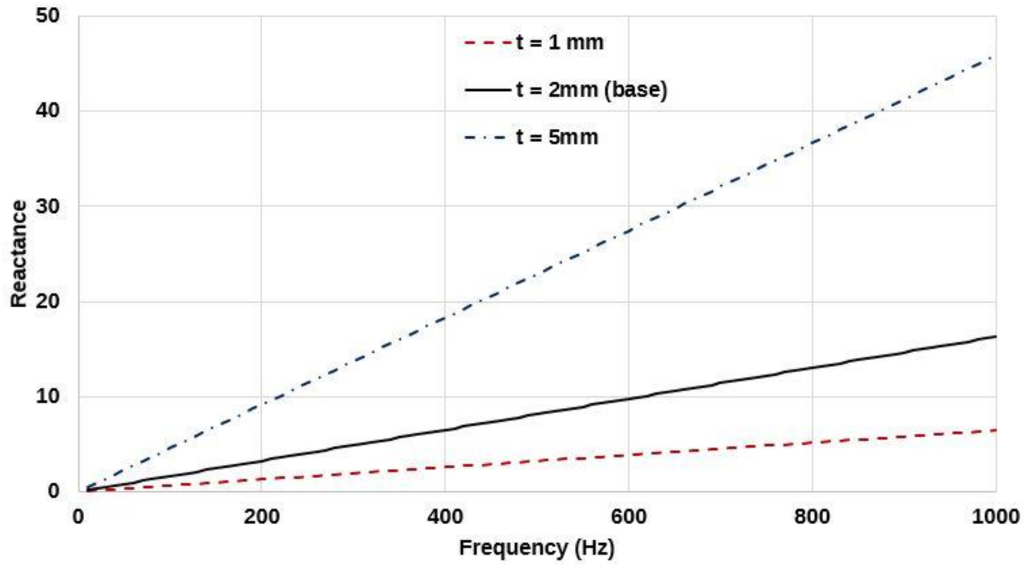

Figure 9: Variation of reactance with liner wall thickness (t)

Figures 9 and 10 shows the effect of the liner wall thickness and hole diameter on reactance, respectively. The values are varied as mentioned in Table 1. It can be observed from Fig. 9 that as the liner wall thickness increases, the reactance increases linearly because the reactance is directly proportional to the wall thickness as can be observed in Eq. (2).

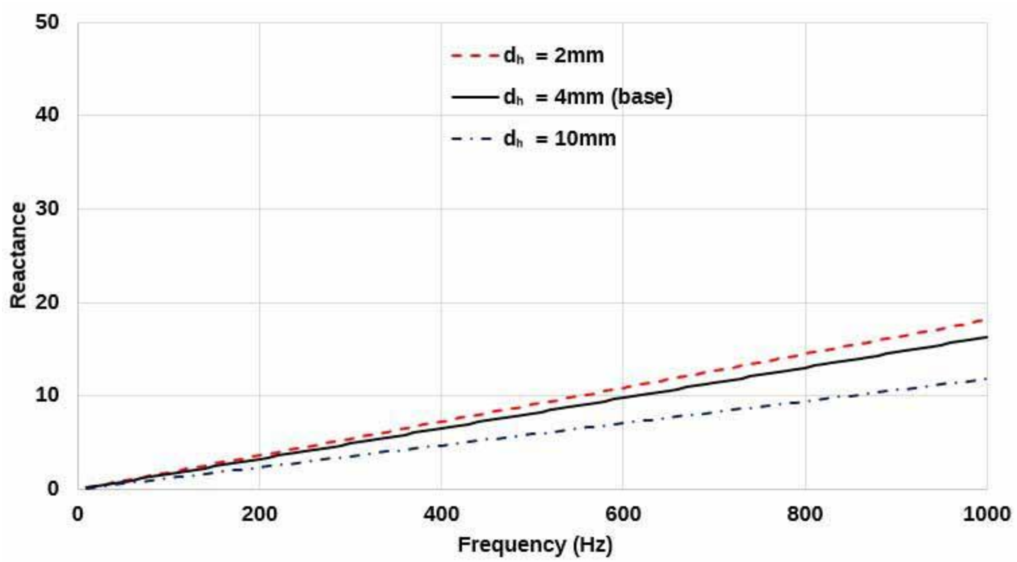

Figure 10: Variation of reactance with hole diameter (d_h)

On contrast, as seen in Fig. 10 the reactance decreases with an increase in the hole diameter even though the reactance is proportional to the hole diameter as in Eq. (2). This is because the porosity σ, which is equal to *OAR* in this case, is a function of square of the hole diameter. This makes the reactance inversely proportional to the hole diameter and hence the decreasing trend in impedance is observed with increasing hole diameter.

4. Summary

A finite element methodology was developed to estimate the impedance of single hole, multiple hole samples in a virtual impedance tube and cylindrical liner (CTR) with single hole. Based on the numerical results of impedance tube with a single hole, a new end correction coefficient was proposed. Next, a comparison of the results of a single hole and multiple hole configuration was made and it was inferred that estimation of impedance based on a single hole with porosity using unit cell configuration is not appropriate if the multiple hole configuration is not a regular pattern. Parametric studies have been conducted to study the effect of liner wall thickness and hole diameter for CTR with single hole configuration. Further, the effect of curvature is studied based on results of CTR with a single hole; and it was found that curvature effects are not significant for plane wave mode propagation.

Acknowledgement

The work shown in this paper has been conducted as part of Gas Turbine Enabling Technology (GATET) initiative supported by Gas Turbine Research Establishment (GTRE), Bangalore. This financial support is gratefully acknowledged.

References

1 Lahiri, C. *Acoustic performance of bias flow liners in gas turbine combustors*, Doctor of Engineering Dissertation, Transport and Machine Systems, TU Berlin, (2014).
2 Lawn, C. The acoustic impedance of perforated plates under various flow conditions relating to combustion chamber liners, *Applied Acoustics*, **106**, 144-154, (2016).
3 Jones, M., Tracy, M., Watson, W. and Parrott, T. Effects of liner geometry on acoustic impedance, In *8th AIAA/CEAS Aeroacoustics Conference & Exhibit*, Breckenridge, Colorado, 17-19 June, (2002).
4 Jones, M., Parrott, T. and Watson, W. Comparison of acoustic impedance eduction techniques for locally-reacting liners, In *9th AIAA/CEAS Aeroacoustics Conference and Exhibit*, Hilton Head, South Carolina, 12-14 May, (2003).
5 Jones, M., Watson, W. and Nark, D. Effects of flow profile on educed acoustic liner impedance, In *16th AIAA/CEAS Aeroacoustics Conference*, Stockholm, Sweden, 07-09 June, (2010).
6 Bellucci, V., Flohr, P. and Paschereit, C.O. Numerical and Experimental Study of Acoustic Damping Generated by Perforated Screens, *AIAA Journal*, **42**(8), pp.1543-1549, (2004).
7 Hughes, I.J. and Dowling, A.P. The absorption of sound by perforated linings, *Journal of Fluid Mechanics*, **218**, 299-335, (1990).
8 Dassé, J., Mendez, S. and Nicoud, F. Large-eddy simulation of the acoustic response of a perforated plate. In *14th AIAA/CEAS Aeroacoustics Conference*, Vancouver, British Columbia, Canada, 05-07 May, (2008).
9 Eldredge, J., Bodony, D. and Shoeybi, M. Numerical investigation of the acoustic behavior of a multi-perforated liner. In *13th AIAA/CEAS Aeroacoustics Conference*, Rome, Italy, 21- 23 May, (2007).
10 Mazdeh, A. *Damping parameter study of a perforated plate with bias flow*, Doctoral dissertation, School of Engineering, University of Dayton, (2012).
11 Andreini, A., Bianchini, C., Facchini, B., Simonetti, F. and Peschiulli, A. Assessment of numerical tools for the evaluation of the acoustic impedance of multi-perforated plates, In *ASME 2011 Turbo Expo: Turbine Technical Conference and Exposition*, Vancouver, British Columbia, Canada, 6–10 June, (2011).
12 Sullivan, J.W. and Crocker, M.J. Analysis of concentric-tube resonators having unpartitioned cavities, *The Journal of the Acoustical Society of America*, **64**(1), pp.207-215, (1978).
13 Sullivan, J.W. A method for modelling perforated tube muffler components. II. Applications, *The Journal of the Acoustical Society of America*, **66**(3), pp.779-788, (1979).
14 Melling, T.H. The acoustic impedance of perforates at medium and high sound pressure levels, *Journal of Sound and Vibration*, **29**(1), 1-65, (1973).
15 Altair University. NA. *Element Quality and Checks*. [Online.] available: http://www.altairuniversity.com/wpcontent/uploads/2012/04/Student_Guide_211 233.pdf
16 MSC Software Company, Actran 17.0 User's Guide, (2016).
17 Munjal, M. L., *Acoustics of Ducts and Mufflers*, John Wiley & Sons, Hoboken, NJ (2014).